



Cite this: *Lab Chip*, 2015, 15, 4273

Received 9th August 2015,
Accepted 11th September 2015

DOI: 10.1039/c5lc00953g

www.rsc.org/loc

Microfluidic multiplexed partitioning enables flexible and effective utilization of magnetic sensor arrays

Daniel J. B. Bechstein,^a Elaine Ng,^b Jung-Rok Lee,^a Stephanie G. Cone,^c Richard S. Gaster,^{bd} Sebastian J. Osterfeld,^e Drew A. Hall,^{fg} James A. Weaver,^f Robert J. Wilson^h and Shan X. Wang^{*fh}

We demonstrate microfluidic partitioning of a giant magnetoresistive sensor array into individually addressable compartments that enhances its effective use. Using different samples and reagents in each compartment enables measuring of cross-reactive species and wide dynamic ranges on a single chip. This compartmentalization technique motivates the employment of high density sensor arrays for highly parallelized measurements in lab-on-a-chip devices.

Following the decade old trend of “Moore’s Law”,¹ feature sizes in integrated circuits (ICs) continue to shrink. The same arguments of technological advances and economics support shrinking sensor size and integrating more sensors per silicon chip, with the goal of large-scale sensor arrays that feature highly parallelized multiplexing, high speed, and lower overall costs.

Giant magnetoresistive (GMR) sensors are one of the most promising sensor technologies for protein diagnostics.² Arrays of 64 GMR sensors have been demonstrated to perform multiplexed protein detection on a single chip,³ and current research targets an even larger number of sensors per array.⁴ However, large-scale sensor arrays’ utility and bioassay flexibility is limited by concentration mismatch and dynamic range constraints as well as inter-assay cross-reactivity between biological analytes and reagents from different assays.⁵ Thus, only a subset of protein assays of interest can be performed in parallel on a single sensor array chip without exceeding cross-reactivity or dynamic range constraints. The dynamic range of sensors can be improved through

optimized particle selection, sensor design, and readout circuitry, which reduces the constraints on concentration ranges.^{3,6–9} The cross-reactivity between analytes and reagents is a more stringent constraint for accurate readout that cannot be solved by increased sensor electronic performance, but needs to be taken care of at its source – the biochemical binding stage early in the detection workflow. Antibody cross-reactivity^{5,10,11} and aberrant protein–protein interactions¹² are two undesired sources of assay cross-reactivity. This cross-reactivity becomes a problem in sensor-based multiplex assays where the goal is to integrate many tests onto a small sensing region, and leads to challenges and issues with assay reliability. Common approaches deal with cross-reactivity similar to well-based assays, where each assay is performed in a separate well. This separation prevents cross-reactivity by design: the cross-reactive assays are separated onto different chips, ultimately requiring an increased number of sensor chips rather than parallel processing on a single chip. However, this multi-chip separation approach defeats the purpose of scaling up sensor arrays to accommodate more sensors, as the number of potential cross-reactive reagent pairs increases quadratically with the number of assays performed in parallel.

While cross-reactivity is already problematic in the current 64 sensor array, larger-scale sensor arrays will only exacerbate the problem. To enable the effective use of large-scale sensor chips, it is necessary to separate cross-reactive species on the sensor chip. This separation requires technology that can interface and segregate the sensor at the sensor pitch length scale. Microfluidic technology has been demonstrated interfacing a single GMR sensor,^{13,14} therefore it is a particularly promising approach in partitioning the sensor surface into different compartments and addressing individual sensor compartments with reagents. A diverse range of microfluidic immunoassays have been implemented using paper, polydimethylsiloxane (PDMS) and other materials.^{2,15–18} Of these technologies, PDMS chips are especially useful for interfacing sensors¹⁴ and enable automation and miniaturization.^{16,19}

^a Mechanical Engineering, Stanford University, Stanford, CA 94305, USA

^b Bioengineering, Stanford University, Stanford, CA 94305, USA

^c Biomedical Engineering, University of North Carolina, Chapel Hill, NC 27514, USA

^d Medicine, Harvard University, Cambridge, MA 02138, USA

^e MagArray Inc., Milpitas, CA 95035, USA

^f Electrical Engineering, Stanford University, Stanford, CA 94305, USA.

E-mail: sxwang@stanford.edu

^g Electrical and Computer Engineering, UCSD, La Jolla, CA 92093, USA

^h Material Science, Stanford University, Stanford, CA 94305, USA

Here, we compartmentalize a biosensor array using microfluidic channels, separate cross-reactive assays into different compartments and demonstrate cross-reactivity-free measurement of otherwise cross-reactive assays. Overcoming these constraints, this approach enables flexible and effective utilization of magnetic sensor arrays. Additionally, the microfluidic compartmentalization can be used to separate species with incompatible dynamic ranges. In the GMR sensor array, all 64 sensors can be individually functionalized with specific capture antibody or control using a robotic spotter, enabling completely independent immunoassays on each sensor on the same chip (Fig. 1).

Detection is based on a magnetic immunoassay, where a sandwich immunoassay is performed directly on the GMR sensor. Captured protein is labelled with magnetic particles (Miltenyi Biotec μ MACS Streptavidin MicroBeads), which are magnetized in an applied magnetic field. The particle's stray magnetic field changes the magnetization orientation of the underlying GMR sensor, which yields a change in electric resistance that is read out with low noise electronics and correlates to the quantity of bound magnetic particles and thus protein analyte (see details in ref. 3 and 20). In immunoassays on the GMR sensor platform, pairwise cross reactivity has been observed while performing multiplexed assays with the cancer biomarkers Epidermal Growth Factor Receptor (EGFR), Epithelial Cell Adhesion Molecule (EpCAM), and Transmembrane glycoprotein encoded by the Tacstd2 gene (Trop-2).¹²

We recreated the previously noted cross-reactivity of the individual assay biomarkers by measuring a controlled sample consisting of all three biomarkers: EGFR, EpCAM, and Trop-2, all at 10 ng mL^{-1} in buffer solution on GMR sensors

functionalized with capture antibodies against EGFR, EpCAM, and Trop-2. In separate experiments, either EGFR, EpCAM, or Trop-2 detection antibody was added. The resulting sensor signals for the individually functionalized sensors were recorded and plotted in Fig. 2. Experiments using EpCAM detection antibody did not show any significant cross-reactivity on the EGFR or Trop-2 antibody functionalized sensors. Experiments including EGFR or Trop-2 detection antibodies showed severe cross reactivity: experiments with EGFR detection antibody showed a significant signal from the Trop-2 capture antibody functionalized sensors, experiments with Trop-2 detection antibody showed a large signal from the EpCAM capture antibody functionalized sensors, which was even higher than the Trop-2 capture antibody functionalized sensor's signal. The Trop-2 detection antibody to EpCAM cross-reactivity is assumed to come from antibody cross-reactivity.²¹ The EGFR detection antibody to Trop-2 cross-reactivity is attributed to come from a protein interaction between EGFR and the EGF like domain on the Trop-2 protein.²²

To overcome cross-reactivity, we designed a microfluidic chip, based on standard PDMS Multilayer Soft Lithography (MSL)^{19,23} that interfaces with the GMR sensor array chip, separating it into completely independent compartments (see Fig. 3). Since the microfluidic chip is designed to protrude over the sensor chip's extents (Fig. 1d), a clamping seal can be formed at the microfluidic-to-sensor-chip interface by a custom designed cartridge (see details in ref. 24) that does not interfere with the connection pins. This microfluidic chip separates the 64 sensors in the array into 4 different compartments of 16 sensors each. Each compartment is connected to its individual syringe pump of a standard syringe pump

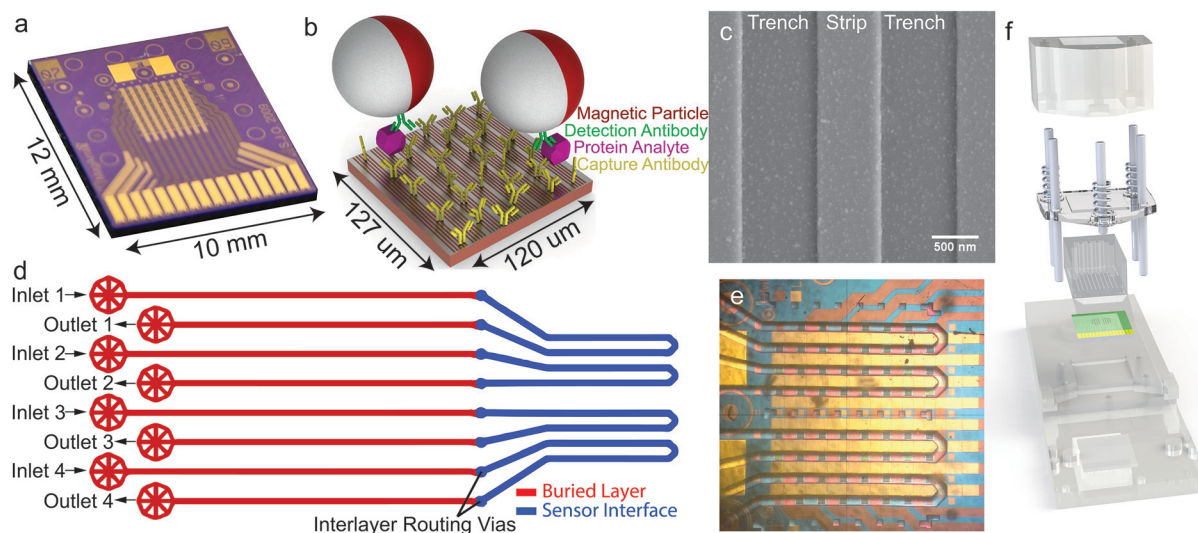


Fig. 1 GMR sensor arrays. a) Sensor array chip containing 64 individual GMR sensors in an 8×8 configuration. b) Schematic of sandwich magnetic immunoassay structure performed directly atop one GMR sensor in the sensor array. c) Scanning electron microscope (SEM) image of magnetic nanoparticles on strips of GMR sensor (used with permission from ref. 6). d) Microfluidic chip schematic (red layers buried, blue layers interfacing chip). e) Microfluidic channels aligned on the sensors and compartmentalize the sensor array into four completely independent, individually addressable compartments. f) Cartridge integrates microfluidic chip and sensor array chip, facilitates alignment, and provides pressure seal between microfluidic channels and sensor array.

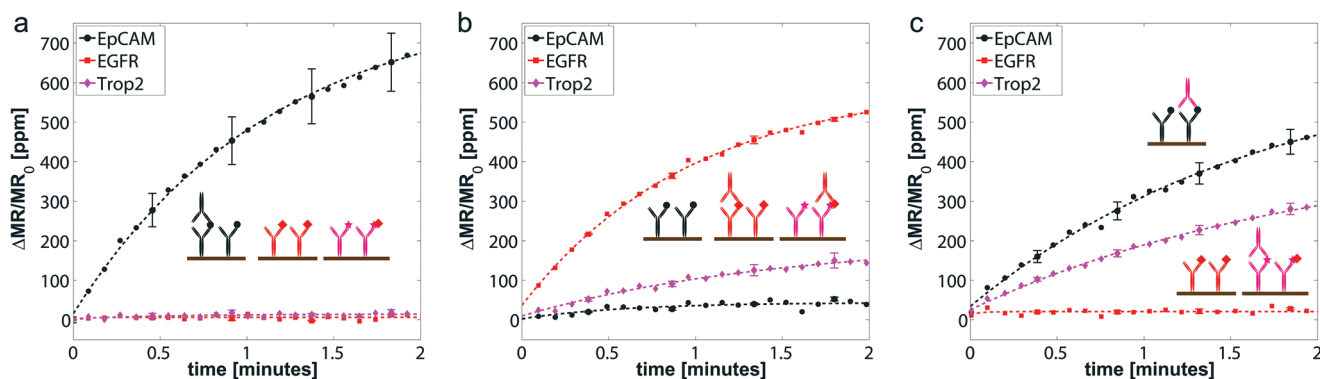


Fig. 2 Detection antibody cross-reactivity in EpCAM, EGFR, and Trop-2 assays. a) EpCAM assay, b) EGFR assay, and c) Trop-2 assay measurements. Sensors were functionalized with the three relevant capture antibodies (Anti-EpCAM, Anti-EGFR, and Anti-Trop-2; curves are labelled by specific analyte of capture antibody). All three analytes are present in each channel, but only the specific detection antibody is added, depending on the channel either: a) EpCAM, b) EGFR, or c) Trop-2). Error bars denote sample standard deviation ($n = 4$), plotted every 5th data point. Insets: schematic of detection antibody cross-reactivity in sandwich assays.

system (NE-1800, New Era Pump Systems) that delivers analytes and reagents to the sensors of that compartment at a flow rate of $2 \mu\text{L min}^{-1}$.

We performed the cross-reactive EGFR, EpCAM, and Trop2 assays with the same controlled sample solution (of all three protein biomarkers mixed together at 10 ng mL^{-1}). Each assay is separated in an isolated compartment (sensor signals plotted in Fig. 3a) with only the specific assay detection

antibody present (see Fig. 3a inset). Thus by design the cross-reactivity is avoided.

More broadly speaking, this compartmentalization allows multiple samples to be assayed on a single GMR sensor array chip. To demonstrate this, a series dilution assay of C-reactive protein (CRP) was measured (Fig. 3b). Thus sample dilutions can be targeted to match the concentration range to the dynamic range of the sensor.

Conclusions

This compartmentalization approach allows the separation and, by design, cross-reactivity free measurement of analytes on a single sensor array chip, which would otherwise show cross-reactivity. Additionally, this approach allows measurement of multiple analyte samples on the same chip, including serial dilutions for overcoming dynamic range limitations. Overall, the microfluidic integration and compartmentalization approach allows a more flexible and effective use of existing sensor arrays, motivates the employment of larger-scale sensor arrays for highly parallelized diagnostics, and adds a microfluidic interface for higher degrees of automation of sample delivery assays.

Acknowledgements

This work was supported by Physical Science Oncology Center (U54CA143907), Center for Cancer Nanotechnology Excellence (U54CA151459), and BioSTAR through the Stanford Bio-X program. DJBB acknowledges a Stanford Bio-X Graduate Fellowship. SEM images were acquired at the Stanford Nano Shared Facilities. Microfluidic chips were fabricated at the Stanford Microfluidic Foundry. The authors would like to thank Junyi Wang for generating calibration data of GMR sensors.

Notes and references

- 1 G. E. Moore, *Electronics*, 1965, 38, 114–117.
- 2 H. C. Tekin and M. A. M. Gijs, *Lab Chip*, 2013, 13, 4711–4739.

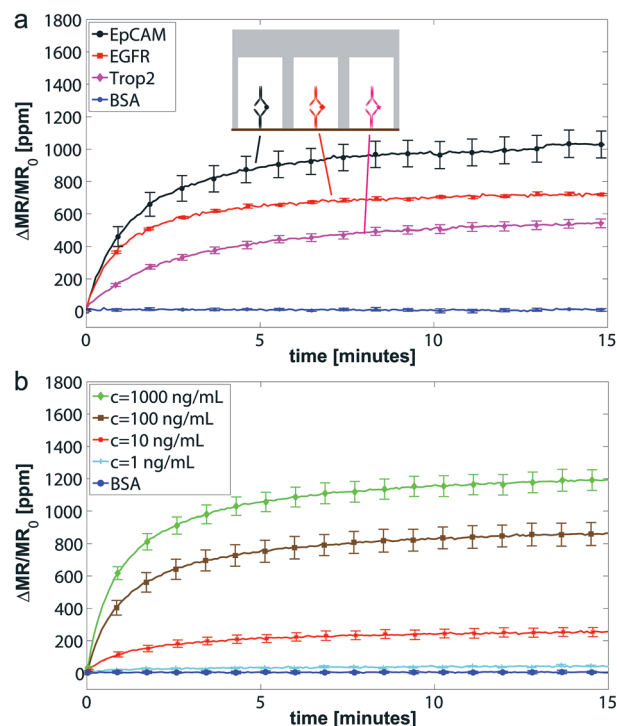


Fig. 3 a) Measurements free of cross-reactivity by separation of assays into different compartments. b) Series dilution CRP assays separated into 4 compartments. Error bars denote sample standard deviation ($n = 4$ for immunoassays in a) and $n = 8$ in b), plotted every 10th data point).

- 3 S. J. Osterfeld, H. Yu, R. S. Gaster, S. Caramuta, L. Xu, S.-J. Han, D. A. Hall, R. J. Wilson, S. Sun, R. L. White, R. W. Davis, N. Pourmand and S. X. Wang, *Proc. Natl. Acad. Sci. U. S. A.*, 2008, **105**, 20637–20640.
- 4 D. A. Hall, R. S. Gaster, K. Makinwa, S. X. Wang and B. Murmann, *IEEE J. Solid-State Circuits*, 2013, **48**, 1290–1301.
- 5 G. A. Michaud, M. Salcius, F. Zhou, R. Bangham, J. Bonin, H. Guo, M. Snyder, P. F. Predki and B. I. Schweitzer, *Nat. Biotechnol.*, 2003, **21**, 1509–1512.
- 6 D. J. B. Bechstein, J.-R. Lee, C. C. Ooi, A. W. Gani, K. Kim, R. J. Wilson and S. X. Wang, *Sci. Rep.*, 2015, **5**, 11693.
- 7 D. A. Hall, R. S. Gaster, T. Lin, S. J. Osterfeld, S. Han, B. Murmann and S. X. Wang, *Biosens. Bioelectron.*, 2010, **25**, 2051–2057.
- 8 R. S. Gaster, D. A. Hall, C. H. Nielsen, S. J. Osterfeld, H. Yu, K. E. Mach, R. J. Wilson, B. Murmann, J. C. Liao, S. S. Gambhir and S. X. Wang, *Nat. Med.*, 2009, **15**, 1327–1332.
- 9 D. Kim, F. Marchetti, Z. Chen, S. Zaric, R. J. Wilson, D. A. Hall, R. S. Gaster, J.-R. Lee, J. Wang, S. J. Osterfeld, H. Yu, R. M. White, W. F. Blakely, L. E. Peterson, S. Bhatnagar, B. Mannion, S. Tseng, K. Roth, M. Coleman, A. M. Snijders, A. J. Wyrobek and S. X. Wang, *Sci. Rep.*, 2013, **3**, 2234.
- 10 G. MacBeath, *Nat. Genet.*, 2002, **32**, 526–532.
- 11 B. Schweitzer, S. Roberts, B. Grimwade, W. Shao, M. Wang, Q. Fu, Q. Shu, I. Laroche, Z. Zhou, V. T. Tchernev, J. Christiansen, M. Velleca and S. F. Kingsmore, *Nat. Biotechnol.*, 2002, **20**, 359–365.
- 12 R. S. Gaster, D. A. Hall and S. X. Wang, *Nano Lett.*, 2011, **11**(7), 2579–2583.
- 13 J. Loureiro, P. Z. Andrade, S. Cardoso, C. L. Da Silva, J. M. Cabral and P. P. Freitas, *Lab Chip*, 2011, **109**, 2255–2261.
- 14 M. Muluneh and D. Issadore, *Lab Chip*, 2014, **14**, 4552–4558.
- 15 L. Gervais, M. Hitzbleck and E. Delamarche, *Biosens. Bioelectron.*, 2011, **27**, 64–70.
- 16 G. M. Whitesides, *Nature*, 2006, **442**, 368–373.
- 17 C. D. Chin, V. Linder and S. K. Sia, *Lab Chip*, 2007, **7**, 41–57.
- 18 A. W. Martinez, S. T. Phillips, G. M. Whitesides and E. Carrilho, *Anal. Chem.*, 2010, **82**, 3–10.
- 19 M. A. Unger, H.-P. Chou, T. Thorsen, A. Scherer and S. R. Quake, *Science*, 2000, **288**, 113–116.
- 20 S. X. Wang and G. Li, *IEEE Trans. Magn.*, 2008, **44**, 1687–1702.
- 21 G. Eisenwort, J. Jurkin, N. Yasmin, T. Bauer, B. Gesslbauer and H. Strobl, *J. Invest. Dermatol.*, 2011, **131**, 2049–2057.
- 22 D. Fong, G. Spizzo, J. M. Gostner, G. Gastl, P. Moser, C. Krammel, S. Gerhard, M. Rasse and K. Laimer, *Mod. Pathol.*, 2008, **21**, 186–191.
- 23 J. C. McDonald, D. C. Duffy, J. R. Anderson, D. T. Chiu, H. Wu, O. J. A. Schueller and G. M. Whitesides, *Electrophoresis*, 2000, **21**, 27–40.
- 24 D. J. B. Bechstein and S. X. Wang, in *Proceedings MicroTAS*, 2014.